Millimeterwave Imaging Sensor Nets: A Scalable 60-GHz Wireless Sensor Network

Munkyo Seo, Bharath Ananthasubramaniam, Mark Rodwell, and Upamanyu Madhow

Department of ECE, University of California, Santa Barbara, CA, 93106 USA

***Abstract* — We report first experimental results on the prototype for a novel wireless sensor network that offers both data collection and localization capability. The proposed architecture assumes minimal sensor functionality in analogy to optical imaging, and suits very large-scale sensor networks. The use of millimeterwave beacon, wide in frequency and narrow in space, enables accurate flight-time (and thus distance) and angular location measurement with the employment of non-coherent 2-D matched filtering. Design and characterization of a 60-GHz prototype system, including low-cost passive sensor, is presented.**

***Index Terms* — sensor network, localization, beam steering.**

I. Introduction

Sensor networks provide distributed information collection and transmission, and are useful for many industrial, environmental or military applications. A large number of sensors are randomly or systematically deployed over a certain field for local data gathering. Such information is transferred to a final destination in a multi-hop fashion among neighboring sensors by locally forming an ad-hoc network. For a complete information map, a certain kind of positioning is also necessary in most cases, i.e. each sensor node needs to provide its own location information as well. External positioning capability such as GPS may be used for this purpose. This conventional approach is widely used in many practical applications, but scalability issue arises when the number of sensor nodes is very large (e.g. >1,000). First, multi-hop data transmission is not very efficient in a large scale network. Second, the cost of each sensor may not scale down commensurately with the scale of network because of the minimum required intelligence (for e.g. positioning and ad-hoc networking). The complexity of sensor also strongly correlates with power consumption. Although modern CMOS technologies enable efficient signal processing, the collective cost and energy expenditure may be unacceptable for very large scale sensor networks.

The authors proposed a new approach to address scalability issue [1]-[2], and this paper presents first experimental results with 60-GHz prototype system and sensors. Section II reviews the system architecture. Following sections present the system design and experimental characterization results based on short-range (<12m) indoor radio experiment.

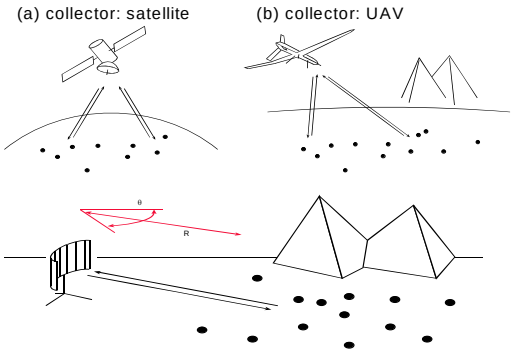

Fig. 1. Typical realizations of the proposed imaging sensor networks with three different kinds of information collector

II. Imaging Sensor Network Architecture

The motivation behind the proposed architecture is best described by *simplistic sensors*: stripped of their complexity to retain only essential functionality without any geolocation (positioning) or networking capability. This will enable ultimate cost and energy efficiency in favor of a very large scale network. The system complexity (or functionality) is instead moved to an information *collector*, whose spatially narrow radio beam selectively activates a subset of sensor nodes. Fig.1 illustrates three representative scenarios. In either case, the collector beam sequentially scans a sensor field (2D or 3D in general). Illuminated sensors respond to the beacon by appropriately modulating and sending it back to the collector. The collector, upon completing a full scan, acquires necessary information map across sensor field. The location of each sensor can also be accurately determined by using a wide bandwidth, spatially narrow beacon in analogy to radar. The return signal, however, also carries local data from possibly a number of sensors, unlike conventional radar. Furthermore, sensors intentionally shift the frequency of the received beam to differentiate their transmission signal with direct ground return or environmental reflections. This necessitates non-coherent signal processing unlike conventional synthetic aperture radar (SAR). The proposed sensor net can also be interpreted as a virtual *imaging* network: image map is drawn from reflected light by a large number of target pixels.

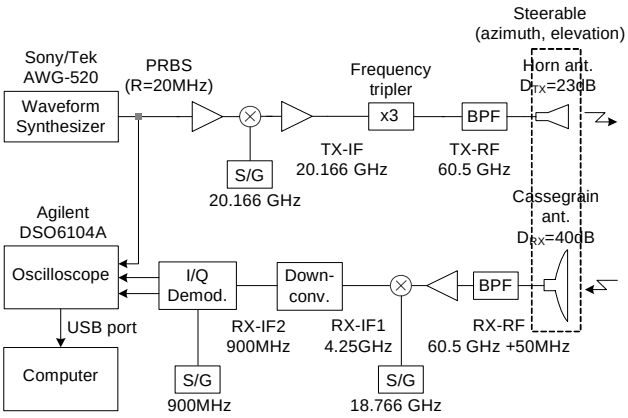

Fig. 2. Block diagram of 60-GHz prototype collector. The oscilloscope digitizes the reference PRBS and received I and Q signals.

III. Prototype Collector

Fig.2 shows a simplified block diagram of the experimental 60-GHz collector. It consists of three functional blocks: up-down converter, steerable high-gain antennas and digital signal processing routine.

A. 60-GHz Up/Down Converter

The input to the up/down converter is a *range code*, which is basically a wide-band signal having a sharp autocorrelation peak. By taking cross-correlation between its transmit and receive copy, and by finding the location of peak, the relative distance between the collector and sensor can be estimated. In this initial work, pseudo-random bit sequence (PRBS) signal is adopted. The chip-rate (CR) and length of PRBS determines raw range resolution and the sensor field size, respectively. With higher CRs, a single chip travels shorter distance in the air, and thus the correlation peak becomes sharper, providing finer range resolution. One PRBS period must be long enough to round-trip the most distance sensor (otherwise a single correlation peak will correspond to two or more different ranges, causing ambiguity). We chose the *CR* and length to be 20-MHz and 2^6-1, respectively. A single chip thus round-trips $c/(2CR) = 7.5m$ of range distance (*c*: the speed of light). The PRBS repeats itself for every $(2^6 - 1)/CR = 3.15us$, and this is enough for unique determination of the range up to 472.5*m*.

The PRBS is upconverted to TX-IF (20.166 GHz) followed by frequency triplication to reach 60.5 GHz. The tripler output power is 8dBm. The transmitted beam, once received by a sensor, is shifted in frequency by 50-MHz (to filter out ground returns), and received by a high-gain collector antenna. A harmonic mixer and block down-converter translates the received beam down to the first IF (RX-IF1=4.25GHz) and second IF (RX-IF2=900MHz), respectively. The final I/Q demodulator output is digitized by a multi-channel oscilloscope for subsequent digital signal processing. A copy of transmit PRBS code is also captured for timing (and hence range) reference.

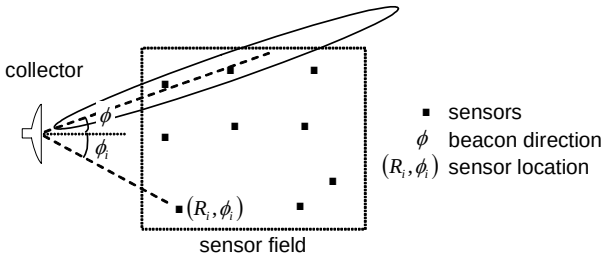

Fig. 3. Imaging sensor net geometry in angular coordinate

B. Steerable High-gain Antennas

High-gain antennas are beneficial for the proposed imaging sensor nets for two reasons. First, higher-gain antennas have proportionately narrower beam angles, yielding finer angular resolution. This is seen from the following relationship.

$$D \approx 4\pi/(\Theta_1\Theta_2),$$

where D, Θ_1 and Θ_2 are the antenna gain and half-power beamwidth (in radian) in orthogonal directions, respectively. Second, transmit power density is proportional to the antenna gain. The collector beacon therefore reaches further with higher gain antenna. The gain of TX and RX antenna for the prototype collector in Fig.2 is D_{TX}=23dB and D_{RX}=40dB, respectively. Their half-power beamwidth is approximately 14 degree and 2 degree, respectively. They are mounted on a motorized positioner so that the beam can be steered in azimuth and elevation with sub-degree accuracy.

C. Digital Signal Processing: Localization and Demodulation

The role of collector signal processing is first, to accurate determine the location of sensors, and second, to reliably demodulate local sensor data at the same time. Only localization process is described in this section, although the current prototype is also capable of data demodulation.

Fig.3 illustrates the sensor network coordinate assuming a beam-steerable collector. Let $s(t)$ the range code, and $r(t,\phi)$ the collector receive signal as a function of azimuth angle ϕ and time *t*. Assume the collector is at origin, and a single sensor is located at (R_1, ϕ_1). $r(t,\phi)$ is then represented as

$$r(t,\phi) = A(\phi - \phi_1)s(t - R_1/2c) + n_1(t),$$

where $A(\phi)$ and $n_1(t)$ is the antenna gain function (AGF) and Gaussian noise, respectively. The maximum-likelihood (ML) estimate of the sensor location, $(\tilde{R}_1, \tilde{\phi}_1)$, can be obtained from the observation $r(t,\phi)$ by

$$(\tilde{R}_1, \tilde{\phi}_1) = \arg\max_{(\tilde{R},\tilde{\phi})} \left\langle A(\phi - \tilde{\phi}), \left| \left\langle r(t,\phi), s(t - \tilde{R}/2c) \right\rangle_t \right| \right\rangle_\phi, \quad (1)$$

where $\langle\cdot\rangle_t$ and $\langle\cdot\rangle_\phi$ is taking cross-correlation in *t* and ϕ, respectively. Equation (1) is essentially 2-D matched filtering,

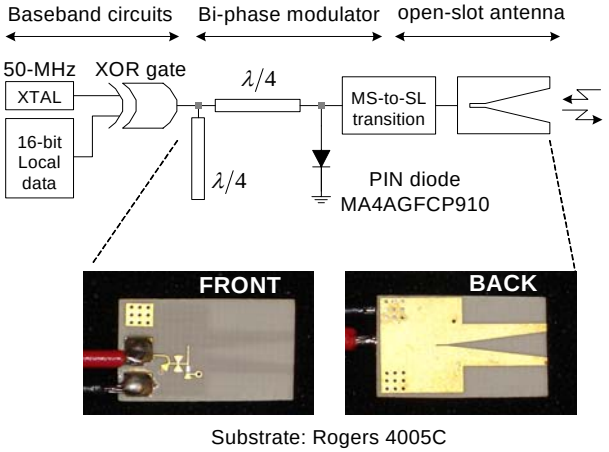

Fig. 4. A prototype 60-GHz low-cost passive sensor with a wideband antenna and BPSK modulator. The size of RF circuitry is ~15mm by 10mm.

[3] but only the magnitude is taken from the range correlation output. This is because the phase of $r(t,\phi)$ is unknown to the collector. The AGF $A(\phi)$ is equal to the cascade of collector TX and RX antenna. For the present prototype, $A(\phi)$ is almost equal to RX antenna (40dB cassegrain) pattern since the TX antenna (23dB horn) has a much wider 3-dB beamwidth.

IV. Prototype Sensor

The essential functionality of imaging net sensors is to receive, modulate and re-radiate the 60-GHz beacon. The construction of communication circuits in 60-GHz band presents a certain level of difficulty in low-cost implementation. One quarter-wavelength at 60-GHz is approximately 0.5mm on a $\varepsilon_r = 4$ substrate. This is rather small compared to lithographic tolerance (~1mil=0.025mm) and minimum line width/spacing (4~5mil=0.1~0.125mm) in standard low-cost PC board manufacturing (finer technologies may be sought, e.g. LTCC, but at a potentially significant cost penalty.). Sensor RF circuitry (antenna, matching network, etc) will therefore suffer from detuning. RFIC integration will be cost-effective, but the sensor antenna will still need to be off-chip due to its considerable size. Further, dielectric loss and skin effects introduce significant signal attenuation at 60-GHz band, especially with low-cost substrates. All above considerations suggest that the sensor RF circuitry must be simple and robust against manufacturing error.

Fig.4 shows the first 60-GHz prototype sensor block diagram. The RF circuitry is implemented on a low-cost Rogers 4005C substrate (thickness=0.2mm and $\varepsilon_r = 3.38$). A linearly-tapered open-slot antenna (LTSA) is chosen for the present work in favor of its wideband operation and frequency-independent geometry, and hence insensitivity to manufacturing error. The slot feed line, microstrip line and their transition is carefully designed under 5-mil resolution constraint. The designed antenna has >10 GHz bandwidth

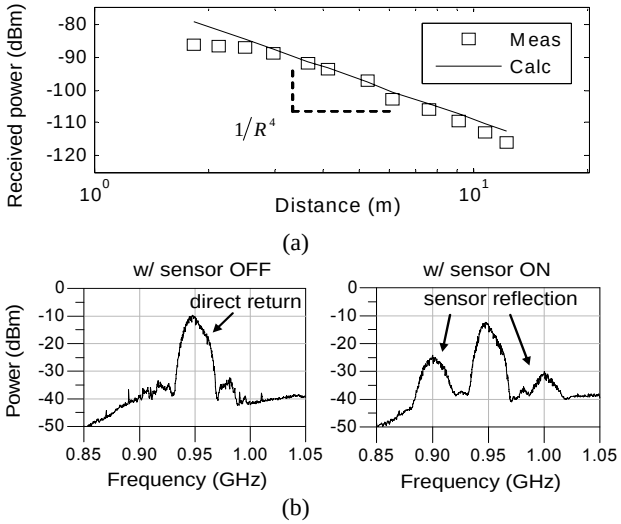

Fig. 5. (a) Collector input power versus range. (b) Collector RX-IF2 spectrum with a sensor at ~3m. Sensor return signal is seen at 50MHz off the 20-MHz PRBS beacon directly reflected from indoor environments. Collector antenna is aimed at the sensor in both cases.

centered at 60GHz. Its half-power beamwidth is approximately 40 degree with 7dB of realized gain accounting for loss.

The collector beam is received by a LTSA terminated by a PIN diode. The input bias turns on and off the PIN diode, presenting two impedance states with approximately 180 degree phase difference. The beacon is hence reflected with either 0 or 180 degree relative phase shift, and eventually re-transmitted toward the collector. 16-bit local data and 50-MHz shifting LO (to avoid direct ground returns) are simultaneously imposed on diode bias through a XOR gate. Current prototype consumes ~7mA of dc current from a 3-V supply to forward-bias the PIN diode. The dc power consumption will, however, significantly drop (e.g. uW level) if the entire circuit (except for the LTSA) is implemented on silicon.

The current prototype sensor is *passive* without any active RF amplification. Its reflected power entirely depends on the collector transmit power. On one hand, this suits well with the simplistic sensor approach; the sensor has minimal RF functionality, and corresponding implementation loss can be compensated by raising the beacon power. On the other hand, passive sensors are practically unsuitable for longer range communication (e.g. >1km). Scaled CMOS devices (e.g. 90-nm node or below) will again provide low-cost millimeterwave amplification and help to scale up the sensor network.

V. Radio Link Characterization

The round-trip radio link between the collector and passive sensor (Fig.4) is governed by the following relationship.

$$\frac{P_r}{P_t} = D_{TX} D_{RX} D_{sens}^2 G_{sens} \left(\lambda_{up}\lambda_{down}\right)^2 \frac{e^{-2\alpha R}}{(4\pi R)^4}. \quad (2)$$

In (2), P_r and P_t are the collector receive and transmit power, respectively. D_{TX}, D_{RX} and D_{sens} are collector TX, RX and sensor antenna gain, and λ_{up} and λ_{up} are up- and down-link wavelength, respectively. R is the distance and α is atmospheric attenuation constant, 6~16dB/km in 60-GHz unlicensed band. G_{sens} models modulation loss in the sensor (<-3dB). Other sources of power attenuation include matching loss, polarization loss, etc. Note from (2) that the received power quickly drops as $1/R^4$. To revert to more desirable $1/R^2$ dependency, the sensor must operate in a power-limited regime with sufficiently high RF gain. In this case, the maximum communication range is the square of $1/R^4$ case. Fig.5 (a) compares the collector receive power between measurement and calculation. Fig.5 (b) shows the in-band received spectrum with and without sensor reflection.

VI. Sensor Localization and Demodulation

Fig.6 illustrates range measurement process and data demodulation example at a fixed angular position. Next, range localization results of a single sensor case are summarized in Fig.7. Standard deviation error is ~0.1m which corresponds to 1.3% of a single chip flight distance. Finally, the collector beam is swept across ~15.6 degree azimuth in steps of 0.625 degree, with the elevation fixed. Then, 2-D matched filtering is performed as discussed in Section III.*C*. Fig.8 shows the resulting matched filter output with one and two sensors. Note that the localization performance, both in radial and angular direction, improves with a longer observation, since uncorrelated noises average out.

VI. Conclusion

We have demonstrated the basic link, localization and demodulation performance of a prototype 60GHz wireless sensor network, based on a virtual-imaging approach. Further characterization and the system enhancement are under way.

References

[1] B. Ananthasubramaniam and U. Madhow, "Virtual radar imaging for sensor networks," in *Proceedings of the third international symposiumon on IPSN*, Berkeley, California, USA: ACM Press, New York, April 2004, pp. 294–300.

[2] U. Madhow, M. Rodwell, B. Ananthasubramaniam, M. Seo, and P. Park, "Imaging sensor nets: An rfid-inspired framework for million node sensor networks," in *Book of Extended Abstracts, International Workshop on RFID and Wireless Sensors*, Kanpur, India, Nov 2005, pp. 32–33. [Online]. Available: http://www.iitk.ac.in/ee/RFIDWS/rfweb/Book of Extended Abstracts Final.pdf

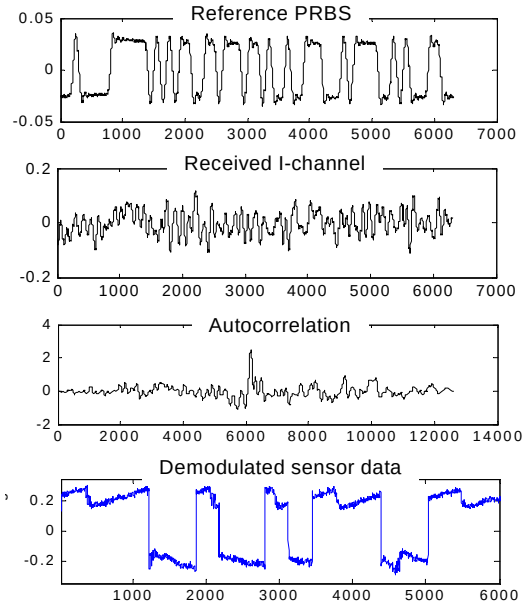

Fig. 6. Example of range measurement and data demodulation: The reference PRBS (up) is used as a timing reference. The received signal (upper middle) is correlated with the reference to yield a sharp autocorrelation peak (lower middle). The location of the peak indicates relative distance of the sensor. The bottom plot is the final matched filter output showing demodulated sensor data at 1kbps.

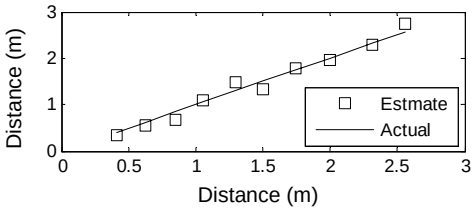

(a)

Fig. 7. Range measurement results with a single sensor at a fixed angular position.

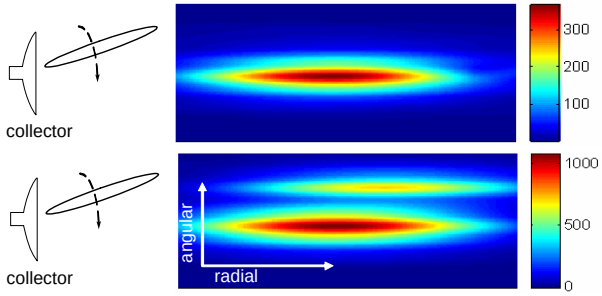

Fig. 8. 2-D localization result: Reconstructed sensor field map from the magnitude of 2-D matched filter output with a single sensor (up) and two sensors (down). The peak(s) on each map indicate(s) the most probable sensor location(s). Note: maps not to scale; actual field size is 12m by 0.6m.

[3] B. Ananthasubramaniam and U. Madhow, "On localization performance in imaging sensor nets," submitted to *IEEE Trans. Signal Processing*.